NPL REPORT
CIRM 46

NPL contribution to an international comparison of 24.5 keV neutron fluence measurements

David J Thomas

June 2001

June 2001

NPL contribution to an international comparison of 24.5 keV neutron fluence measurements

David J Thomas

Centre for Ionising Radiation Metrology
National Physical Laboratory, Teddington, Middlesex

Abstract

This report contains details of the experimental procedure and the analysis techniques used by NPL during an international comparison of neutron fluence production and measurement in the energy region around 24 keV. The exercise involved the calibration of three spheres from a Bonner sphere set in terms of their fluence response to 27.4 and 24.6 keV neutrons produced using the $^{45}Sc(p,n)^{45}Ti$ reaction.

ISSN 1369-6793

National Physical Laboratory
Teddington, Middlesex, United Kingdom, TW11 0LW

Approved on behalf of Managing Director, NPL, by
Dr Martyn Sené, Head, Centre for Ionising Radiation Metrology

CONTENTS

Page

1. Introduction

This report describes the analysis of measurements, made at NPL during September and October 1995, to determine the response of three Bonner spheres to monoenergetic neutrons at 24.6 keV and 27.4 keV. The work was part of a CCEMRI (Comité Consultatif pour les Etalons de Mesure des Rayonnements Ionisants)[*] comparison performed to determine the ability of various national laboratories to produce known neutron fluences with energies around 24 keV, and to use these fluences to determine the responses of neutron sensitive devices in this energy region.

Monoenergetic neutrons in the range from 8 keV to about 30 keV are produced at NPL using the $^{45}Sc(p,n)^{45}Ti$ reaction. Protons from the NPL 3.5 MV Van de Graaff accelerator are used to bombard thin (20 $\mu g\ cm^{-2}$) scandium targets evaporated onto 0.5 mm thick backing disks. For the measurements described here the discs were of tungsten, although later work has indicated that tantalum has certain advantages. The cross section of the reaction exhibits resonance peaks in the region just above the threshold, which is at 2908 keV, and the energies of these peaks are well known[(1)]. On gradually increasing the proton bombarding energy from threshold these peaks can be identified, from the count rate in a neutron detector positioned in front of the target, by comparison with plots of the yield as a function of proton energy as given, for example, in reference 1. A typical yield curve as a function of proton energy, as measured with the NPL standard long counter (LC) positioned at 0^o to the proton beam direction, is given in Figure 1. The energy of the proton beam is determined from the frequency of an NMR probe situated within the field of the energy selection magnet in the Van de Graaff beam line. Although the proton energy is roughly proportional to the square of the NMR frequency, a plot of yield against frequency, which can quickly and easily be produced as the experiment proceeds, provides a similar picture to Figure 1, and one from which the required peak can easily be identified.

The procedure to produce a 27.4 keV neutron fluence at 0^o to the direction of the proton beam involves locating the appropriate resonance, and then maintaining the proton beam energy at this value. This requires occasional, very small, adjustments to the Van de Graaff accelerator controls, as and when required, to compensate for any slight energy drifts. These drifts are recognised by a decrease in the yield from the target per unit proton beam current.

Neutrons of 24.6 keV are produced at 35^o to the direction of the proton beam when the neutron energy at 0^o is 27.4 keV. Tables, based on relativistic calculations of the reaction kinematics, have been produced giving the energy at any angle for a whole range of incident proton bombarding energies.

The three Bonner spheres used in this comparison had polyethylene moderator diameters of 22", 32", and 92" (6.4 cm, 8.9 cm, and 24.1 cm), and the central thermal neutron detector was a Centronic model SP9 spherical ^3He proportional counter. (The polyethylene spheres were made to exact inch diameters, and these values are used as labels for the spheres throughout this report.) Signals from the ^3He counter were processed using conventional NIM electronic modules (see the Appendix). A discriminator level was set in the pulse height spectrum between the noise signals and neutron induced events, where the count rate is very low, and all events above the discriminator level were recorded in a scaler unit.

[*] The committee name has since changed to: Comité Consultative des Rayonnements Ionisants (CCRI)

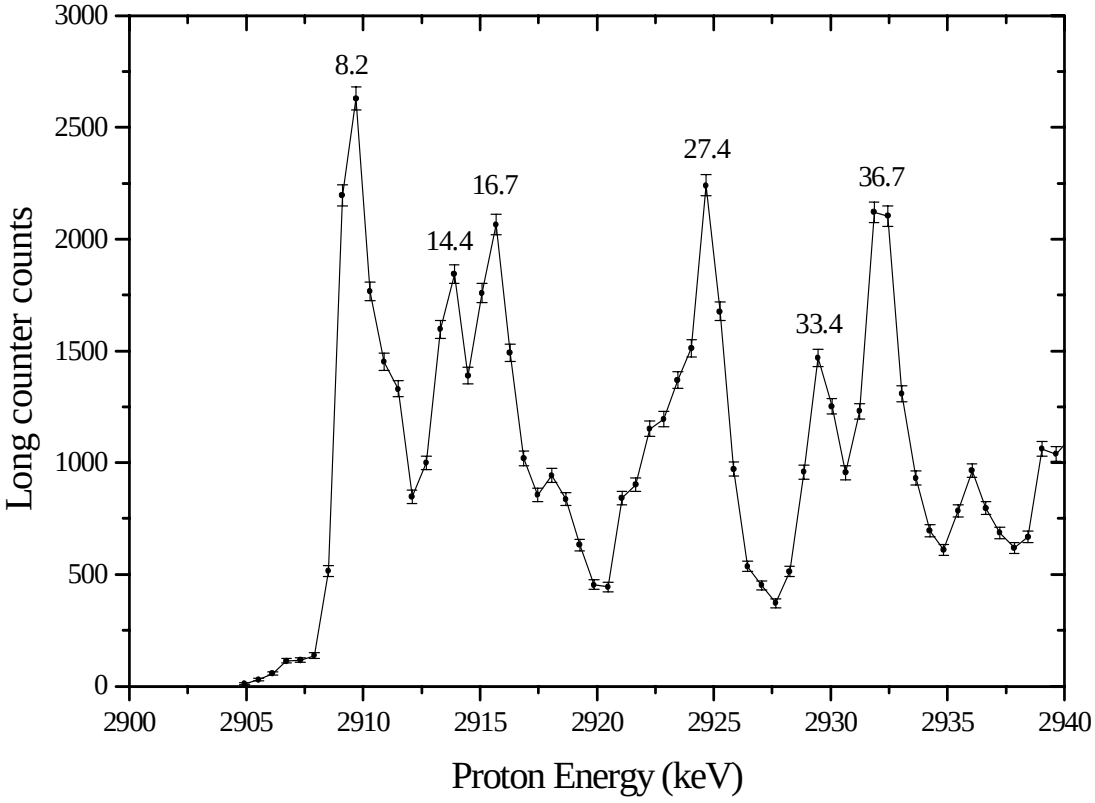

Figure 1. NPL standard long counter counts, as a function of proton beam energy, for a charge of 1 mC on the target. The energies of the resonances are shown in keV.

The neutron fluence was determined using the NPL standard long counter whose neutron detection efficiency has been determined by a combination of methods including calibration with radionuclide sources of accurately known emission rate[(2)].

Corrections for room and air in-scattered neutrons detected in both the Bonner spheres and the long counter were made using the shadow cone technique. This allows the direct fluence from the neutron producing target to be determined by a straightforward subtraction technique. Other corrections need to be applied for neutrons produced in the target backing, and for neutrons produced by the proton beam striking slits in the beam line at the exit from the energy selection magnet. This latter component is small since the magnet is situated about 16 m from the target, and there is some shielding around the slits. Nevertheless, a correction needs to be made because of the low yield from the Sc(p,n) reaction. This low yield makes the measurements generally difficult; in particular, it is very time consuming to acquire reasonable counting statistics, even for efficient neutron detecting devices such as the long counter and the Bonner spheres.

A stable monitor device is required to provide a link between the fluence measurement with the long counter and the irradiation of the Bonner spheres. A large moderator detector, mounted in a fixed position on the wall of the experimental room, was used for this purpose. This detector, consisting of banks of BF_3 proportional counters in a polyethylene moderator slab, is known as the SLAB detector. It has three layers of detectors at three different depths in the polyethylene, but only the top layer, designated SLAB1, was used in these measurements because of the low penetrating power of the low energy neutrons in the polyethylene. Throughout the measurements, the beam current on the target was also recorded in terms of the pulses from a current integrator. This quantity does not provide a good monitor of the Sc(p,n) neutrons, because the reaction yield is very critically dependent on the

proton beam energy which can vary slightly, but it does provide a good monitor for neutrons produced in the target backing and at the slits.

A more extensive listing of the raw data, and a more detailed description of the analysis procedure, is presented in this document than would normally be the case in a report of an instrument response measurement. There are two reasons for this. Firstly it provides a complete and permanent record of all the data acquired and how it was processed. This should provide guidance for subsequent similar measurements at NPL, not only to the experimental method and analysis, but also to the magnitude of the counts to be expected in monitors and the long counter. Secondly, the approach allows interested parties to study the analysis process in detail.

2. The analysis procedure

As noted above, in the present set of measurements, the long counter and the Bonner spheres respond to neutrons from a number of sources other than the Sc(p,n) reaction, and all of these sources need to be identified and accounted for. The formalism for doing this is given below.

The various components of the fluence seen by a neutron detector at the measurement position are denoted by, Φ, with a subscript to indicate where the neutrons have come from. Fluences which originate initially from Sc(p,n) reactions in the target are written without superscript. Fluences which originate from all other reactions, in the target or elsewhere along the beam-line, are indicated by a superscript of a single 'dash', i.e. Φ'. Summed fluences which include neutrons from **both** the above indicated sources are written with a double 'dash', i.e. Φ''.

The character, Ψ, with similar subscripts and superscripts, denotes fluences seen by the neutron monitor, i.e. SLAB1.

All fluences indicated with a single 'dash' are assumed to be proportional to the beam current and hence the beam current integrator is a measure of their intensity.

The effects of target scattering are ignored in the initial analysis, and also perturbations in SLAB1 readings caused by scatter from different sized devices at the measurement position.

All the fluence contributions seen by a detector and by the monitor are listed below where the term in-scatter refers to neutrons detected after scatter by the walls or ceiling of the calibration room, equipment within the room, or the air.

Detector		Monitor
Φ_D	Direct neutrons from Sc(p,n) reaction	Ψ_D
Φ_{DI}	In-scattered neutrons from Sc(p,n) reaction	Ψ_{DI}
Φ'_C	Direct neutrons from reactions in the target backing	$\Psi'_{C.}$
Φ'_{CI}	In-scattered neutrons from reactions in the target backing	Ψ'_{CI}
Φ'_L	Direct neutrons from sources elsewhere along beam line	$\Psi'_{L.}$
Φ'_{LI}	In-scattered neutrons from sources along beam line	Ψ'_{LI}

(Φ'_L is that component of the fluence from reactions of the beam with the beam-line which is removed by a shadow cone. For the 35^o measurements it will be zero, for the 0^o measurement it should be small, but may be non-zero.)

During calibrations measurements were made of:

the total fluence at the detector using the Sc(p,n) target	Φ''_T - without shadow cone
the scattered fluence at the detector using the Sc(p,n) target	Φ''_{SC} - with shadow cone
the fluence at the detector using a background target	Φ'_{BT} - without shadow cone
the scattered fluence at the detector using a background target	Φ'_{BSC} - with shadow cone

Note that the term "using a background target" may mean employing a separate target, identical in all respects except for the presence of a scandium layer, or it can mean the use of the scandium target at a beam energy below the reaction threshold, see later sections for further details.

Corresponding readings for the neutron-detecting monitor were also recorded. Writing out in full the components of the fluence seen by the detector and the neutron monitor one gets:

for the detector:

$$\Phi''_T = \Phi_D + \Phi_{DI} + \Phi'_C + \Phi'_{CI} + \Phi'_L + \Phi'_{LI}$$

$$\Phi''_{SC} = \Phi_{DI} + \Phi'_{CI} + \Phi'_{LI}$$

$$\Phi'_{BT} = \Phi'_C + \Phi'_{CI} + \Phi'_L + \Phi'_{LI}$$

$$\Phi'_{BSC} = \Phi'_{CI} + \Phi'_{LI}$$

for the monitor:

$$\Psi''_T = \Psi_D + \Psi_{DI} + \Psi'_C + \Psi'_{CI} + \Psi'_L + \Psi'_{LI}$$

$$\Psi''_{SC} = \Psi_D + \Psi_{DI} + \Psi'_C + \Psi'_{CI} + \Psi'_L + \Psi'_{LI} + \Psi''_S$$

$$\Psi'_{BT} = \Psi'_C + \Psi'_{CI} + \Psi'_L + \Psi'_{LI}$$

$$\Psi'_{BSC} = \Psi'_C + \Psi'_{CI} + \Psi'_L + \Psi'_{LI} + \Psi''_S$$

For completeness, a term, Ψ''_S, has been included above for scattering from the shadow cone into the monitor.

When performing subtractions to remove the contribution to an instrument reading corresponding to an unwanted fluence component it is important to make sure an appropriate monitor is being used, i.e. one which is appropriate to the fluences being subtracted.

The quantity required from a measurement, with either the long counter or a Bonner sphere is the response to Sc(p,n) neutrons per unit monitor count, and this is given by:

$$\frac{(\Phi''_{T} - \Phi'_{BT})}{(\Psi''_{T} - \Psi'_{BT})} - \frac{(\Phi''_{SC} - \Phi'_{BSC})}{(\Psi''_{SC} - \Psi'_{BSC})} \qquad (1)$$

In performing the four subtractions in brackets in equation (1) the fluence contributions which are removed by the subtraction are proportional to the beam current. The only exception is Ψ''_{S} which is very small and, provided all measurements are made with the proton beam energy fairly well tuned to the resonance, should subtract reasonably well when taking (Ψ'_{SC} - Ψ'_{BSC}). Assuming all the measurements are performed for an equal number of current integrator pulses then the fluences subtracted, i.e. Φ'_{BT}, Φ'_{BSC}, Ψ'_{BT}, and Ψ'_{BSC} should not be re-normalised in any way. Thus mean values of the counts per unit current integrator corresponding to these fluences should be obtained and subtracted directly from the corresponding values of Φ''_{T}, Φ''_{SC}, Ψ''_{T}, and Ψ''_{SC}.

3. Presentation of the raw data for 0° (27.4 keV) measurements.

A number of different scandium targets were used for the measurements. Despite constant air-cooling, and the use of relatively low beam currents (# 15 μA), the bombardment tended, with time, to destroy the targets. The tungsten backing >blistered=, and the blister tended to flake and break off. (Later investigations indicated that this effect does not occur for tantalum backings.) All the useable data were obtained from just two targets, designated Sc95B and Sc95C.

The data in Tables 1 and 2 give an idea of the magnitude of the counts in the various devices, and also allow the variation of the raw counts per current integrator pulse in the different measurements to be compared. In this way the extent to which it was possible to stay tuned to the resonance in the Sc(p,n) yield and hence maintain a constant energy can be examined.

Each datum in these tables represents an average over a number of cycles, typically 5 or 6 cycles, but varying from 2 to more than 10. Each cycle represents the counts for 2000 current integrator pulses. Since the current integrator was set to 10^{-6} coulomb per pulse, this corresponds to an integrated charge of 2 mC. Uncertainties were calculated both from the spread of the data, and by assuming Poisson statistics. Because of the extreme sensitivity of the yield to the proton beam energy, the uncertainty from the spread was usually the greater of the two and is the value usually quoted. Occasionally, however, when the number of cycles was small, the uncertainty from assuming Poisson statistics was the larger, in which case the Poisson statistics value is quoted. Repeat measurements were made whenever time allowed, most noticeably on 8.9.1995 when four measurements were made for both the NPL long counter and the 92" sphere.

The Bonner spheres were positioned on lightweight supports to minimise scattering from the support into the sphere. Instruments were positioned at essentially the same distances from the neutron producing target in all experiments, so that data taken on different days could be compared directly. The long counter was at 151 cm, the spheres at 120 cm, and the SLAB detector is fixed at about 8.5 m from the target. All data values were corrected for dead-time losses, although in most cases these were negligibly small.

The important data as far as consistency of the final results is concerned is not the counts per unit current integrator pulse, but the ratio of the detector reading to the SLAB1 neutron monitor counts. These ratios are shown in Table 3. Because the figures in this table represent

ratios between two neutron detectors, the values should not be sensitive to the variation in the target yield. Uncertainties calculated from the spread of the data and from assuming Poisson statistics tended to agree better, but the slightly pessimistic approach of taking the largest value was still adopted in all cases.

All the uncertainties quoted in this report are standard uncertainties providing an uncertainty estimate at a confidence level of approximately 68%

Table 1. 0^{o} measurements: NPL long counter and sphere average counts for 2000 current integrator pulses averaged over a number of cycles.

Date	**Target**	**Detectors**			
		NPL LC	**2½"**	**3½"**	**9½"**
Sc(p,n) total					
8.9.95	Sc95B	4751 ∀ 31	416 ∀ 9	1136 ∀ 32	283 ∀ 12
"	Sc95B	3800 ∀ 44	417 ∀ 8	1346 ∀ 24	347 ∀ 13
"	Sc95B	4536 ∀ 48			438 ∀ 9
"	Sc95B	4220 ∀ 84			455 ∀ 11
4.10.95	Sc95C	3522 ∀ 162	397 ∀ 12	1318 ∀ 31	373 ∀ 13
"	Sc95C	3807 ∀ 36			
Sc(p,n) shadow cone					
8.9.95	Sc95B	168 ∀ 6	89 ∀ 5	191 ∀ 6	50 ∀ 4
4.10.95	Sc95C	148 ∀ 7	87 ∀ 5	164 ∀ 12	41 ∀ 2
Background total (Number of cycles given in square brackets)					
27.9.95	W95B	32 ∀ 2[9]	6 ∀ 1[6]	11 ∀ 1[5]	10 ∀ 1[7]
4.10.95	W95B	32 ∀ 3[5]	5 ∀ 1[5]		10 ∀ 1[5]
% of Sc(p,n) total		0.8%	1.4%	0.9%	2.7%
Background shadow cone					
27.9.95	W95B	14 ∀ 2[4]	6 ∀ 1[3]	9 ∀ 2[5]	5 ∀ 1[3]
4.10.95	W95B	16 ∀ 2[4]	5 ∀ 1[5]		4 ∀ 1[5]
% of Sc(p,n) cone		10%	6.2%	5.1%	9.9%

Table 2. 0^{o} measurements**:** SLAB1 counts for 2000 current integrator pulses averaged over a number of cycles. Each datum is associated with the corresponding datum for a detector as shown in Table 1.

Date	Target	Detector at measurement position			
		NPL LC	**2½"**	**3½"**	**9½"**
Sc(p,n) total					
8.9.95	Sc95B	866 ∀ 12	854 ∀ 11	689 ∀ 18	529 ∀ 16
"	Sc95B	680 ∀ 16	820 ∀ 10	853 ∀ 13	653 ∀ 46
"	Sc95B	843 ∀ 48			810 ∀ 14
"	Sc95B	746 ∀ 19			820 ∀ 19
4.10.95	Sc95C	653 ∀ 14	825 ∀ 18	847 ∀ 18	754 ∀ 23
"	Sc95C	700 ∀ 15			
Sc(p,n) shadow cone					
8.9.95	Sc95B	703 ∀ 44	796 ∀ 15	841 ∀ 12	819 ∀ 14
4.10.95	Sc95C	642 ∀ 18	797 ∀ 18	748 ∀ 18	750 ∀ 22
Background total					
27.9.95	W95B	41 ∀ 4	43 ∀ 3	43 ∀ 3	40 ∀ 2
4.10.95	W95B	39 ∀ 3	40 ∀ 3		44 ∀ 4
% of Sc(p,n) total		5.5%	5.1%	5.3%	5.8%
Background shadow cone					
27.9.95	W95B	48 ∀ 5	49 ∀ 4	44 ∀ 3	49 ∀ 4
4.10.95	W95B	45 ∀ 3	39 ∀ 3		43 ∀ 3
% of Sc(p,n) cone		7.1%	5.5%	5.5%	5.9%

Table 3. Ratio of NPL long counter and sphere counts to SLAB1 for 0^o measurements.
NB Data is **without** background subtraction

Date	Target	Detectors			
		NPL LC	**2½"**	**3½"**	**9½"**
Sc(p,n) total					
8.9.95	Sc95B	5.50 ∀ 0.09	0.487 ∀ 0.011	1.65 ∀0.06	0.534 ∀ 0.028
"	Sc95B	5.59 ∀ 0.14	0.509 ∀ 0.011	1.58 ∀ 0.03	0.533 ∀ 0.032
"	Sc95B	5.40 ∀ 0.32			0.541 ∀ 0.011
"	Sc95B	5.66 ∀ 0.16			0.556 ∀ 0.016
	Means	5.54 ∀ 0.07[b]	0.498 ∀ 0.011[a]	1.59 ∀ 0.03[a]	0.544 ∀ 0.008[b]
4.10.95	Sc95C	5.39 ∀ 0.17	0.481 ∀ 0.010	1.56 ∀ 0.02	0.495 ∀ 0.009
"	Sc95C	5.44 ∀ 0.13			
	Mean	5.42 ∀ 0.10[b]			
Sc(p,n) shadow cone					
8.9.95	Sc95B	0.241 ∀ 0.010	0.111 ∀ 0.005	0.228 ∀ 0.007	0.061 ∀ 0.005
4.10.95	Sc95C	0.231 ∀ 0.012	0.110 ∀ 0.007	0.218 ∀ 0.011	0.055 ∀ 0.003

All means have been derived using $1/\sigma^2$ weighting
a uncertainty from formula for weighted mean
b uncertainty from square root of reciprocal of sum of weights

The data in Table 3 do not always correspond exactly to the values which would be obtained by dividing a datum in Table 1 by the corresponding datum in Table 2. This is because each value in Table 1 or Table 2 represents a mean of a number of measurement cycles, whereas the corresponding datum in Table 3 represents the mean of the **ratio** values for these cycles.

4. Background corrections for 0^o measurements.

Measurements to provide estimates of the neutron production in the target backing material, i.e. the target background corrections, can be performed in one of two ways:

1) using the scandium target and arranging the beam energy to be below the Sc(p,n) threshold,

or

2) using a matching blank >background= target, i.e. one having just the tungsten backing.

Option 2 has advantages in that one is not risking 'burning out' a scandium target, BUT one must have an exactly matching tungsten blank, i.e. one which produces the same number of neutrons as the backing of the scandium target used. A measurement using either approach also includes the background contribution from neutron production at the slits. A shadow cone measurement is needed to separate out this component, see the discussion in Section 2.

All the useable data with scandium targets were obtained with two targets Sc95B and Sc95C. All the useful background target data were obtained with tungsten blank W95B.

For the two scandium targets the backgrounds measured, per 2000 current integrator pulses, by the NPL long counter in the energy region below the Sc(p,n) threshold were:

Sc95B	28 ∀ 2 on 13.9.95
Sc95C	17 ∀ 1 on 21.9.95
Sc95C	18 ∀ 2 on 4.10.95

For the background target the measurements gave:

W95B	32 ∀ 2 on 27.9.95
	32 ∀ 3 on 4.10.95

Thus W95B appears to be a good background target for use with Sc95B.

For Sc95C the background target gives too high a count rate by almost a factor of two for the NPL long counter.

It would appear that for Sc95C the direct component from the tungsten backing must be nearly zero. The value measured in the region below the Sc(p,n) threshold, i.e. 17 or 18 counts per second, is comparable to the value obtained for background target W95B with a shadow cone i.e. 14 or 16 s^{-1} (see Table 1). There is no obvious reason why there should be these variations between backings, and the causes of these variations should be investigated.

Thus, for target Sc95B the background total and background shadow cone values measured with background target W95B were used for subtraction.

For target Sc95C the background shadow cone values measured with W95B were used for both the background total and background shadow cone values. (These will effectively cancel, although there may be some effects because of different count rates per current integrator pulse)

Data for ratios of detector to SLAB1 counts, with background subtraction are given in Table 4 which illustrates the agreement, or otherwise, between the data for various measurements, both on the same day and on a different day with a different target. It allows the consistency of the data to be investigated prior to the next stage of the analysis where the shadow cone subtraction is made, and the average sphere response values are derived based on all the data. If the measurements had been made with the devices at exactly the same distances from the target in all experiments, then the ratios should be constant for a particular sphere. In practice there were some very slight differences, of the order of a few mm, between measurements on different days. The effects of these small differences are, however, much smaller than the

measurement uncertainties, so data taken on different days can be compared directly for consistency. Allowance for these small differences in distances were nevertheless made in the final analysis where the sphere counts per unit fluence were derived.

Table 4. Ratio of NPL long counter and sphere counts to SLAB1 for **0°** measurements. **NB** data is now **with** background subtraction

Date	**Target**	**Detectors**			
		NPL LC	**2½"**	**3½"**	**9½"**
Sc(p,n) total					
8.9.95	Sc95B	5.73 ∀ 0.10	0.509 ∀ 0.012	1.75 ∀0.06	0.560 ∀ 0.031
"	Sc95B	5.89 ∀ 0.15	0.529 ∀ 0.012	1.65 ∀ 0.03	0.553 ∀ 0.036
"	Sc95B	5.63 ∀ 0.35			0.558 ∀ 0.012
"	Sc95B	5.93 ∀ 0.17			0.573 ∀ 0.016
	Means	5.80 ∀ 0.07[b]	0.519 ∀ 0.010[a]	1.67 ∀ 0.04[a]	0.562 ∀ 0.009[b]
4.10.95	Sc95C	5.71 ∀ 0.17	0.499 ∀ 0.010	1.63 ∀ 0.03	0.518 ∀ 0.010
"	Sc95C	5.75 ∀ 0.14			
	Mean	5.73 ∀ 0.11[b]			
Sc(p,n) shadow cone					
8.9.95	Sc95B	0.235 ∀ 0.010	0.110 ∀ 0.006	0.229 ∀ 0.007	0.058 ∀ 0.006
4.10.95	Sc95C	0.223 ∀ 0.013	0.109 ∀ 0.007	0.219 ∀ 0.012	0.051 ∀ 0.003

All means have been derived using $1/\sigma^2$ weighting
a uncertainty from formula for weighted mean
b uncertainty from square root of reciprocal of sum of weights

It is noticeable that, for the >total= measurements, the ratios in Table 4, which include background subtraction, are larger than those in Table 3 which do not. This is because the background subtraction is a larger percentage for the SLAB1 readings than of the instrument readings.

The data in Table 5 show the ratios of the corrected detector counts per unit SLAB1 count to the long counter counts per unit SLAB1 count.

Table 5. Ratios of sphere counts to NPL long counter for 0^o data **with** background subtraction

Quantity tabulated is: {X/SLAB1 - X'/SLAB1}/{LC/SLAB1 - LC'/SLAB1}

where: X/SLAB1 is the total count for sphere X over SLAB1 count
X'/SLAB1 is the shadow cone count for sphere X over SLAB1 count
LC/SLAB1 is the total long counter count over SLAB1 count
LC'/SLAB1 is the shadow cone long counter count over SLAB1 count

Target	**Spheres**		
	2½"	**3½"**	**9½"**
Sc95B	0.409 ∀ 0.012 /(5.565 ∀ 0.070) **0.0735 ∀ 0.0023** **(3.1%)**	1.441 ∀ 0.041 /(5.565 ∀ 0.070) **0.259 ∀ 0.008** **(3.1%)**	0.504 ∀ 0.011 /(5.565 ∀ 0.070) **0.0906 ∀ 0.0023** **(2.5%)**
Sc95C	0.390 ∀ 0.012 /(5.507 ∀ 0.110) **0.0708 ∀ 0.0026** **(3.7%)**	1.411 ∀ 0.032 /(5.507 ∀ 0.110) **0.256 ∀ 0.008** **(3.0%)**	0.467 ∀ 0.010 /(5.507 ∀ 0.110) **0.0848 ∀ 0.0025** **(2.9%)**

5. Results for the Bonner sphere responses at 27.4 keV.

From the data in Table 5 the required quantity, i.e. the fluence responses of the Bonner spheres can be derived. By using the known efficiency and effective centre of the long counter at 27.4 keV, the fluence at the position of the long counter can be determined and related to the SLAB1 monitor reading. From the inverse square law dependence of the fluence from the target, the fluence incident on the Bonner spheres can then be determined from the monitor reading. Corrections have to be made for air out-scatter in the path between the target and the sphere or long counter, but this correction is small, and there is an element of cancellation for this correction as the distances are similar.

Table 6 shows the final results for the measurements at 0^o. The uncertainties quoted are counting statistics only and do not include uncertainty components for the determination of the fluence. The differences between the results for the two targets give some idea of the consistency of the measurements.

Table 6. Measured sphere responses, units cm^2, at 0^o, i.e. at 27.4 keV, without target scatter correction or monitor scatter correction

Target	Spheres		
	2½"	**3½"**	**9½"**
Sc95B	0.525 ∀ 0.016 (3.1%)	1.846 ∀ 0.057 (3.1%)	0.651 ∀ 0.016 (2.5%)
Difference	3.6%	0.8%	7.2%
Sc95C	0.507 ∀ 0.019 (3.7%)	1.831 ∀ 0.055 (3.0%)	0.607 ∀ 0.018 (2.9%)
Un-weighted mean	0.516 ∀ 0.012[a] (2.3%)	1.838 ∀ 0.040[a] (2.2%)	0.629 ∀ 0.022[b] (3.5%)

a from square root of inverse of sum of weights
b from formula for uncertainty on weighed mean
NB the uncertainties derive only from statistics and are quoted at 1σ

6. Presentation of the raw data for 35^o (24.6 keV) measurements

The measurements at 35^o involved a very similar set of experiments to those previously described for data acquisition at 0^o. Long counter and Bonner sphere measurements were made separately at this angle, with and without shadow cone, both for a scandium target and for a blank target. The long counter and Bonner sphere data are shown in Table 7 with the corresponding SLAB1 data in Table 8.

One of the reasons for including Tables 7 and 8 is to present a record of the extent to which it was possible to remain precisely at the resonance energy as judged by the constancy of the counts per current integrator pulse. During two runs, one for the 32" sphere and one for the 92" sphere, the beam energy was obviously a little unstable and the instrument and SLAB1 counts per current integrator pulse varied. In the case of the 32" sphere run, consisting of 16 cycles, each one for 2000 current integrator pulses, the SLAB1 counts varied between 867 and 544, a larger variation than in most other measurements. The data from this run were therefore divided into those for which the SLAB1 counts were more than 700 (9 cycles), and those where the SLAB1 counts were less than 700 (7 cycles). These two sets of data were analysed separately and the counts per 2000 current integrator pulses are shown separately in Tables 7 and 8, as are the final results, after background subtraction, in Table 9. From the consistency, within the experimental errors, of the data for the sphere counts per unit SLAB1 count as shown in Table 9, it would appear that variations in the count rate per current integrator of the order given above do not affect the final answer. Similar conclusions can be drawn from the measurement for 92" sphere in which the SLAB1 count rate for 2000 current integrator pulses ranged from 733 to 439 and the data were analysed in two groups, one where the SLAB1 counts were greater than 600 (8 cycles) and one where the counts were less than 600 (10 cycles).

Table 7. 35^{o} measurements: NPL long counter and sphere counts for 2000 current integrator pulses averaged over a number of cycles

Date	Target	Detector			
		NPL LC	**2½"**	**3½"**	**9½"**
Sc(p,n) total					
21.9.95	Sc95C	3803 ∀ 76	401 ∀ 8	1336 ∀ 16	424 ∀ 9
"	Sc95C	3857 ∀ 187	355 ∀ 18	1347 ∀ 21	363 ∀ 12
5.10.95	Sc95C	3333 ∀ 300	370 ∀ 6	1078 ∀ 17*	304 ∀ 13ɜ
"	Sc95C	4187 ∀ 167		835 ∀ 26H	221 ∀ 6&
"	Sc95C				372 ∀ 19
Sc(p,n) shadow cone					
21.9.95	Sc95C	178 ∀ 8	93 ∀ 4	214 ∀ 9	54 ∀ 3
5.10.95	Sc95C	193 ∀ 7	98 ∀ 6	176 ∀ 7	43 ∀ 3
Background total					
9.10.95	W95B	39 ∀ 2	(9 ∀ 3)**	18 ∀ 2	16 ∀ 1
% of Sc(p,n) total		0.9%		1.6%	4.6%
Background shadow cone (No of readings in square brackets)					
9.10.95	W95B	19 ∀ 2 [6]	(9 ∀ 3)**	18 ∀ 2 [6]	18 ∀ 2 [10]
% of Sc(p,n) cone		12%		9.2%	37%

* All slab readings >700
H All slab readings <700
ɜ All slab readings >600
& All slab readings >400 and <600
** No measurement performed, value inferred from 0^{o} data.

Table 8. 35^{o} measurements: SLAB1 counts for 2000 current integrator pulses averaged over a number of cycles

Date	Target	Detector at measurement position			
		NPL LC	**2½"**	**3½"**	**9½"**
Sc(p,n) total					
21.9.95	Sc95C	740 ∀ 14	870 ∀ 24	889 ∀ 13	882 ∀ 11
"	Sc95C	733 ∀ 42	763 ∀ 23	908 ∀ 17	802 ∀ 20
5.10.95	Sc95C	656 ∀ 57	804 ∀ 11	757 ∀ 12*	654 ∀ 16ɔ
"	Sc95C	778 ∀ 46		592 ∀ 14H	490 ∀ 14&
"	Sc95C				723 ∀ 23
Sc(p,n) shadow cone					
21.9.95	Sc95C	759 ∀ 14	809 ∀ 28	929 ∀ 20	904 ∀ 13
5.10.95	Sc95C	765 ∀ 14	843 ∀ 12	792 ∀ 22	641 ∀ 37
Background total					
9.10.95	W95B	45 ∀ 2	(41 ∀ 3)**	39 ∀3	43 ∀ 2
% of Sc(p,n) total		5.9%		5.0%	5.9%
Background shadow cone					
9.10.95	W95B	43 ∀ 3	(41 ∀ 3)**	38 ∀ 3	41 ∀ 2
% of Sc(p,n) cone		5.9%		4.4%	5.6%

* All slab readings >700 ɔ All slab readings >600
H All slab readings <700 & All slab readings >400 and <600
** No measurement performed, value inferred from mean of the other data.

7. Background corrections for 35^o measurements.

Unfortunately, no measurements were performed of the sub-threshold yields at this angle. Also, all the measurements were made with target Sc95C and the background measurements were made with W95B which, subsequent analysis of the 0^o data showed, is not a well-matched background target. Fortunately, however, target Sc95C appears to have a very small target background, possibly even zero since the sub-threshold counts at 0^o with this target are commensurate with those from the background shadow cone measurements which are essentially the background from the beam hitting slits in the beam line.

Thus the background counts used for the long counter and spheres were the readings obtained during the background shadow cone measurement.

The background counts for SLAB1 are a little more difficult to estimate. Background target W95B certainly produces some target background neutrons, as evidenced by both the 0^o and 35^o measurements. SLAB1 will see these target background neutrons, and will see them regardless of whether there is a shadow cone in position or not. In fact the SLAB1 reading per current integrator with a background target should be the same regardless of whether there is a shadow cone in place or not. (Ignoring scatter from the shadow cone into the monitor.) This is borne out by both the 0^o and 35^o data sets in Tables 2 and 8. However, the number of target background neutrons is not large; the 32" and the 92" spheres do not even see them within the statistics. SLAB1 background reading per current integrator pulse for Sc95C should be less than for W95B, but it is difficult to establish by how much. The background subtraction for SLAB1, as estimated with W95B, is only about 5%. Also, there is an extent to which its effect cancels out when the ratio of the sphere counts per unit SLAB1 to the long counter counts per unit SLAB1 is calculated, provided SLAB1 counts per current integrator remain reasonably constant. Thus, for SLAB1 background the counts recorded during the background shadow cone measurements with W95B were used, and the effects of this approximation were assumed to be negligible.

No background data were taken for the 22" sphere and a value had to be derived by analogy with the ratios of the corresponding measurements at 0^o.

The background shadow cone measurement for the 32" and 92" spheres, and to a lesser extent the long counter, are larger than at 0^o. It may be that at 35^o the detectors are exposed to a larger fluence from interactions of the beam with the beam line. The shadow cone will not remove any of these at this angle.

Background corrected long counter and sphere ratios to SLAB1 counts are shown in Table 9 allowing the consistency of the data to be examined prior to the next stage of the analysis. This next step is represented in Table 10 where the sphere to long counter ratios are presented for measurements made on two different days.

Table 9. Ratio of NPL long counter and sphere counts to SLAB1 for 35° measurements. Data is **with** background subtraction

Date	Target	Detectors			
		NPL LC	**2½"**	**3½"**	**9½"**
Sc(p,n) total					
21.9.95	Sc95C	5.42 ∀ 0.12	0.475 ∀ 0.016	1.55 ∀ 0.04	0.483 ∀ 0.013
"	Sc95C	5.57 ∀ 0.15	0.478 ∀ 0.014	1.53 ∀ 0.04	0.453 ∀ 0.013
	Means	5.48 ∀ 0.09[a]	0.477 ∀ 0.011[b]	1.54 ∀ 0.03[b]	0.468 ∀ 0.015[a]
5.10.95	Sc95C	5.40 ∀ 0.11	0.474 ∀ 0.011	1.47 ∀ 0.03*	0.465 ∀ 0.014ɔ
"	Sc95C	5.69 ∀ 0.14		1.48 ∀ 0.04[H]	0.454 ∀ 0.018[&]
"	Sc95C				0.518 ∀ 0.019
	Means	5.51 ∀ 0.14[a]		1.47 ∀ 0.02[b]	0.475 ∀ 0.018[b]
Sc(p,n) shadow cone					
21.9.95	Sc95C	0.220 ∀ 0.012	0.110 ∀ 0.008	0.221 ∀ 0.015	0.042 ∀ 0.006
5.10.95	Sc95C	0.240 ∀ 0.012	0.111 ∀ 0.008	0.210 ∀ 0.010	0.043 ∀ 0.008

All means have been derived using $1/\sigma^2$ weighting

a uncertainty from formula for weighted mean

b uncertainty from square root of reciprocal of sum of weights

* All slab readings >700

H All slab readings <700

ɔ All slab readings >600

& All slab readings >400 and <600

Table 10. Ratios of sphere counts to NPL long counter for **35**^{o} data **with** background subtraction

Quantity tabulated is:		{X/SLAB1 - X'/SLAB1}/{LC/SLAB1 - LC'/SLAB1}
where:	X/SLAB1	is the total count for sphere X over SLAB1 count
	X'/SLAB1	is the shadow cone count for sphere X over SLAB1 count
	LC/SLAB1	is the total long counter count over SLAB1 count
	LC'/SLAB1	is the shadow cone long counter count over SLAB1 count

Measurement date	**Spheres**		
	2½"	**3½"**	**9½"**
21.9.95	0.367 ∀ 0.014 /(5.26 ∀ 0.09) **0.0698 ∀ 0.0029** **(4.2%)**	1.319 ∀ 0.034 /(5.26 ∀ 0.09) **0.251 ∀ 0.008** **(3.2%)**	0.426 ∀ 0.016 /(5.26 ∀ 0.09) **0.0810 ∀ 0.0033** **(4.1%)**
5.10.95	0.363 ∀ 0.014 /(5.27 ∀ 0.14) **0.0689 ∀ 0.0032** **(4.6%)**	1.260 ∀ 0.026 /(5.27 ∀ 0.14) **0.239 ∀ 0.008** **(3.3%)**	0.432 ∀ 0.020 /(5.27 ∀ 0.14) **0.0820 ∀ 0.0044** **(5.4%)**

8. Results for Bonner sphere responses at 24.6 keV.

Applying the same procedure to the 35^{o} data as to the 0^{o} data the final results were obtained and these are shown in Table 11 separately for the measurements made on two different days.

Table 11. Measured sphere responses, units cm^{2}, at 35^{o}, i.e. at 24.6 keV, without target scatter correction or monitor scatter correction

Measurement date	**Spheres**		
	2½"	**3½"**	**9½"**
21.9.95	0.500 ∀ 0.021 (4.2%)	1.790 ∀ 0.057 (3.2%)	0.584 ∀ 0.024 (4.1%)
Difference	1.6%	5.4%	-0.7%
5.10.95	0.492 ∀ 0.023 (4.6%)	1.699 ∀ 0.056 (3.3%)	0.588 ∀ 0.032 (5.4%)
Un-weighted mean	0.496 ∀ 0.016[a] (3.2%)	1.744 ∀ 0.046[b] (2.6%)	0.586 ∀ 0.019[a] (3.3%)

a from square root of inverse of sum of weights
b from formula for uncertainty on weighed mean
NB the uncertainties derive only from statistics and are quoted at 1σ.

9. Uncertainties.

Those standard uncertainties in the ratios of sphere to long counter counts which were determined by statistical means are given in Tables 6 and 11 with the tabulated results for these ratios. The remaining uncertainties are largely common for a particular device, so the uncertainties of Tables 6 and 11 are the appropriate ones to take into consideration when examining the consistency of measurements, for example where different scandium targets were used. Estimates of the remaining uncertainties are given in Table 12. These should be combined in quadrature to give the final uncertainties.

Table 12. Estimates of the non-statistical (type B) uncertainties, all at the 68% (1σ) level

Uncertainty component		**% value**
Long counter efficiency		1.5%
Positioning the long counter		0.3%
Positioning the spheres		0.3%
Effective centre of the long counter ($\forall$ 0.5cm)		0.7%
Monitor calibration stability*		0.5%
Air out scatter (10% of correction)	a) long counter	0.4%
	b) sphere	0.4%
In-scatter correction (6% of correction)	a) long counter	0.3%
	b) 22" sphere	1.3%
	c) 32" sphere	0.8%
	d) 92" sphere	0.7%
Absence of a correction for target scatter		2.0%
Absence of a correction for scatter into the monitor		2.0%
Systematic (type B) uncertainties added in quadrature:		
	a) 22" sphere	3.6%
	b) 32" sphere	3.5%
	d) 92" sphere	3.5%

* Normally the monitor calibration stability uncertainty is assigned a value of 1 or 1.5%, but the results for these measurements represent a mean of four measurements so this component will tend to some extent to be included in the statistical uncertainties.

10. Summary and conclusions

The results presented in Tables 6 and 11 have not been corrected for two important effects. These are: neutron scattering in the target assembly, and the fact that the SLAB1 monitor sees different numbers of scattered neutrons depending on the size of the device at the measurement position. The presence or absence of a shadow cone also effects the SLAB 1 reading, but this is a second order effect involving a correction to a correction (that for room and air in-scatter).

To perform corrections for target scatter neutrons two items of information are required: firstly the spectrum of the scattered component relative to the monoenergetic component, and secondly the response function of the spheres. Neither item of information was available, although reasonable estimates of the sphere response functions could be obtained from the literature e.g. reference 3. The spectrum can, in principle, be calculated using computer codes such as MNCP[4] or the TARGET[5] code from PTB, but this information was not available at the time of the comparison exercise.

In the absence of any available data, an uncertainty component of 2% was added to the total uncertainty to allow for this effect. The use of a long counter, which is essentially a 'flat response' counter, to measure the fluence means that the scattered component was included in the fluence measurement with this device. The spheres also recorded the scattered neutrons, however, with a different efficiency to that for the monoenergetic neutrons. The target scattered neutrons have lower energies than the primary neutrons (except for a very tiny higher energy component for the 35^{o} measurement). For the 2½" and 3½" spheres the response peaks at an energy below the 24 keV region, and so the effect will be a greater fractional increase in the measured reading due to scattered neutrons than for the long counter. The measured response should therefore be too high. For the 9½" sphere the response decreases below the 24 keV region so the effect should be the opposite of that for the other two spheres. The figure of 2% for the additional uncertainty is based on typical corrections at other neutron energies. Target scatter calculations are planned.

Attempts to investigate scattering into the monitor, by keeping the beam conditions as steady as possible and moving a device into the measurement position and then away again, were inconclusive because the fluence production by the target was not sufficiently steady. Repeat experiments are planned. In the meantime additional uncertainty components have been added to the final uncertainty to allow for the absence of these corrections.

Because of the different angular distributions and energies of neutrons from other neutron-producing reactions, the scatter into the monitor cannot be determined using another reaction. Data from measurements with a variety of reactions have, however, indicated that this effect is likely to be of the order of 2%.

For the analysis described here the long counter efficiencies and effective centres were taken from the early work of Hunt[2]. These were the data in general use for determining neutron fluences at the time of the comparison exercise. Since then both experimental and calculational work has been undertaken to verify and improve these data. However, these new data have not yet been fully implemented into the fluence measurement procedure at NPL, mainly because of remaining uncertainties in the determination of the effective centre. The effect of using any new values is expected to be small, of the order of perhaps 2% at most, i.e. within the final uncertainties.

The results of the measurements at 27.4 keV and 24.6 keV, with the full uncertainty estimates, are shown in Table 13 below.

Table 13. Results for the Bonner sphere responses (cm^2) at 27.4 keV and 24.6 keV

Neutron Energy (keV)	Sphere		
	2½"	**3½"**	**9½"**
27.4	0.516 ∀ 0.022 (4.3%)	1.838 ∀ 0.076 (4.1%)	0.629 ∀ 0.031 (4.9%)
24.6	0.496 ∀ 0.024 (4.8%)	1.744 ∀ 0.076 (4.4%)	0.586 ∀ 0.028 (4.8%)
Difference	4.0%	5.4%	7.3%

Uncertainties are total combined values and are quoted at 1σ, i.e. a confidence level of 67%.

From published measurements of Bonner sphere response functions[3] it would be expected, from the shape of the response curve, that the 27.4 keV response should be smaller than the 24.6 keV value for the 22" and 32" spheres, but larger for the 92" sphere. In fact the 27.4 keV values measured were always larger than the 24.6 keV values, probably indicating a systematic effect in the measurements rather than the effect of the energy dependence. The differences due to the two different energies are, however, expected to be small, and since the uncertainties are relatively large, too much significance should not be attached to this fact.

The work described here shows that relatively sensitive neutron measuring devices, such as Bonner spheres, can be calibrated in the energy region around 24 keV using the Sc(p,n) reaction. Because the yield is low, the experiments are more difficult and the statistics much poorer than for the majority of the other neutron-producing reactions presently in use at NPL. One of the difficulties is the need to perform measurements with 'background' targets to correct for neutron production from the target backing. The present work has shown that it is not enough just to have a 'background' target of the same material as the scandium target backing. The yield from such 'background' targets varies, as does the background yield from actual scandium targets. The best option for background measurements is probably to perform them with the actual target at a proton beam energy just below the threshold. If a separate 'background' target is used it must be carefully matched to the actual scandium target.

11. Postscript

The data detailed above were those presented to the evaluator for the CCRI comparison exercise, Dr V.E. Lewis, in the form of a private communication. Subsequently, detailed Monte Carlo calculations of the expected variations of the sphere responses with neutron energy in the 24 keV region became available from Dr B. Wiegel at PTB, Braunschweig. With these data, which are reproduced in the evaluator's initial report on the comparison[6], factors can be derived correcting the 27.4 keV results to the values to be expected at 24.5 keV. Although these corrections are small, being less than the overall uncertainties, they have now been made, and the effects are shown in Table 14, and are illustrated in Figure 2. No corrections have been applied to the 24.6 keV data.

Table 14. Corrected results and statistical uncertainties for the sphere responses (cm^2)

	Sphere		
	2½"	**3½"**	**9½"**
Original 27.4 keV data	0.516 ∀ 0.012 (2.3%)	1.838 ∀ 0.040 (2.2%)	0.629 ∀ 0.022 (3.5%)
Correction to 24.5 keV	1.0272	1.0063	0.9781
Data corrected to 24.5 keV	0.530 ∀ 0.012 (2.3%)	1.850 ∀ 0.040 (2.2%)	0.615 ∀ 0.022 (3.5%)
Original 24.6 keV data	0.496 ∀ 0.016 (3.2%)	1.744 ∀ 0.046 (2.6%)	0.586 ∀ 0.019 (3.3%)
Difference	6.9%	6.1%	4.9%
Un-weighted mean	0.513 ∀ 0.017[a] (3.3%)	1.797 ∀ 0.053[a] (2.9%)	0.600 ∀ 0.016[b] (2.7%)

Uncertainties are quoted at 1σ, i.e. a confidence level of 67%.

a uncertainty from formula for standard error of the un-weighted mean

b uncertainty from square root of inverse of sum of weights

After performing the energy corrections, the two values for a particular sphere should agree reasonably well within just the statistical uncertainties. The non-statistical uncertainties are largely common (correlated) for the measurements at the different energies, and should thus be ignored when making a comparison. There is not complete correlation of the non-statistical uncertainties, for example distance uncertainties are uncorrelated, the uncertainties in target scatter effects are not completely correlated, and neither are those for scatter into the monitor. Nevertheless, there remains a significant fraction of the non-statistical uncertainty which is common to the two energies. For this reason the uncertainties shown in Table 14 and in Figure 2 are purely those due to statistics.

Figure 2 illustrates the degree of agreement between the results, and also the rather small effect of correcting the 27.4 keV data to 24.5 keV. For the 2½" and the 3½" spheres the agreement is made slightly worse by the correction, while the agreement for the 9½" sphere is marginally improved. Considering that there are some small components of the non-statistical uncertainties which are not correlated, and are not included in the uncertainties shown, the overall agreement is quite reasonable. The fact that the 24.6 keV data are always lower than the data taken at 27.4 keV, even after correction to a common energy, is however suspicious, and although it is not possible to exclude statistics as the cause of the differences, the data do point to the possibility of an undetected systematic effect.

The best estimates of the final response values are given, together with their statistical uncertainties in the final row of Table 14. In view of the generally good agreement, and the fact that the uncertainties are similar for both measurements for a particular sphere, the final value is a simple un-weighted mean. For deriving the statistical uncertainties of these values both the standard error of the mean was calculated, and also the uncertainty derived from the square root of the inverse sum of the weights. The value adopted was the larger of these two, although the values derived from the two approaches were broadly compatible.

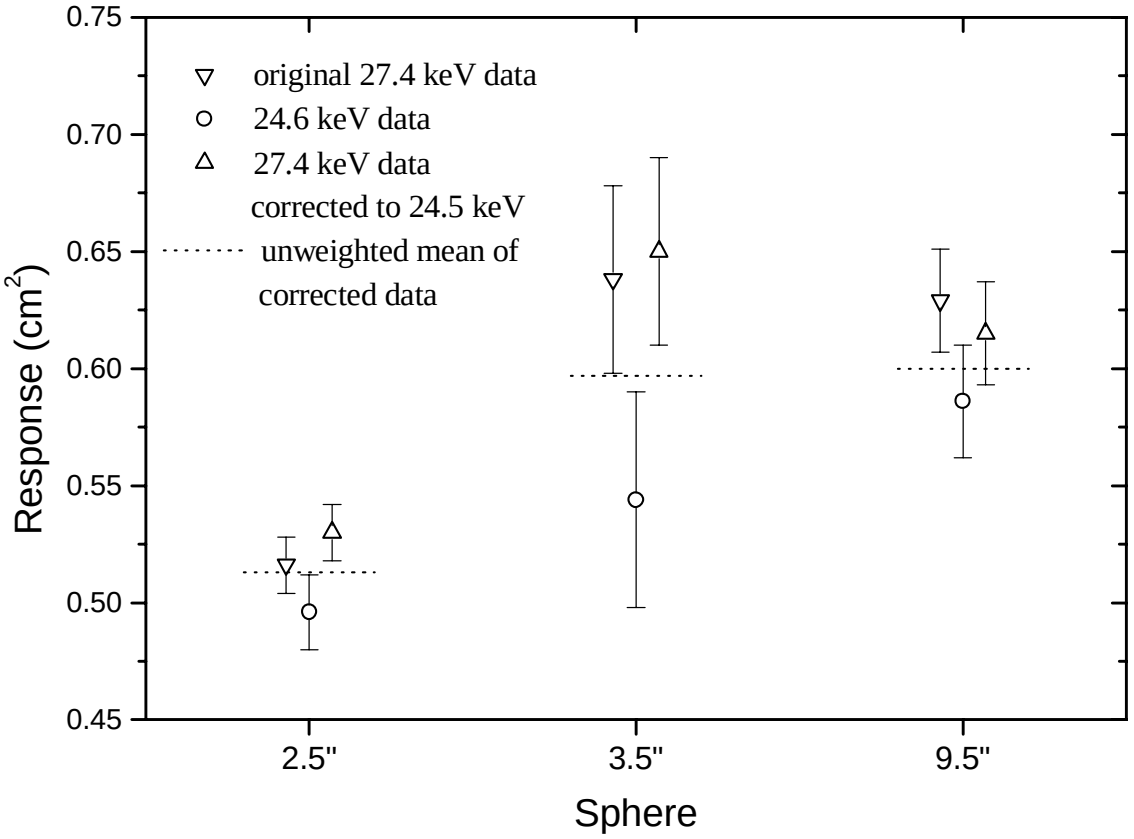

Figure 2. Results for the responses of the three spheres with the statistical uncertainties of the measurements. N.B. the results for the 3½" sphere have been adjusted, by subtracting a factor of 1.2, in order to fit the data on the same plot as the other two responses.

In Table 15 the final values for the responses at 24.5 keV are summarised, together with a breakdown of the uncertainties into statistical (Type A) and non-statistical (Type B) components.

Table 15. Final results and uncertainties for responses of 2½", 3½", and 9½" spheres at 24.6 keV

Sphere	Response (cm^2)	Statistical uncertainty	Non-statistical uncertainty	Combined uncertainty
2½"	0.513	± 0.017 (3.3%)	± 0.018 (3.6%)	± 0.025 (4.9%)
3½"	1.797	± 0.053 (2.9%)	± 0.063 (3.5%)	± 0.082 (4.6%)
9½"	0.600	± 0.016 (2.7%)	± 0.021 (3.5%)	± 0.027 (4.4%)

All uncertainties are quoted at 1σ, i.e. a confidence level of 67%.

Acknowledgements
I would like to thank the operators of the Van de Graaff accelerator for their efficient running of the accelerator and Graeme Taylor who helped with the data acquisition.

References

1. M. Cosack, H. Lesiecki and J.B. Hunt; *Monoenergetic neutrons of energies from 0.5 keV to 40 keV via the reaction $^{45}Sc(p,n)^{45}Ti$,* Proceedings of the Fifth Symposium on Neutron Dosimetry, Munich/Neuherberg 17-21 Sept. 1984, (CEC Luxembourg), Vol. I, pp 597-606, 1985.

2. J.B. Hunt, *The calibration and use of long counters for the accurate measurement of neutron flux density,* NPL Report RS 5, April 1976.

3. A.V. Alevra, M. Cosack, J.B. Hunt, D.J. Thomas and H. Schraube, *Experimental determination of the response of four Bonner sphere sets to monoenergetic neutrons (II),* Radiat. Prot. Dosim. 40, 91-102, 1992.

4. J.F. Breismeister ed., MCNP – *A General Monte Carlo Code for Neutron and Photon Transport*, Los Alamos Report LA-7396-M.

5. D. Schlegel, *Target User's Manual*, Laboratory report, PTB-6.41-98-1, April 1998.

6. V.E. Lewis, *Comparison of 24.5 keV Neutron Fluence Measurements, 1993 – 1996,* NPL Report CIRM 16, December 1998.

Appendix

Electronic modules and settings used for the sphere measurements

Module	Unit	Comments
Detector	SP9 ^{3}He proportional counter	Serial No. SN 9146 195
Preamplifier	Ortec 142 PC	
Main amplifier	Ortec 571	Course gain 20, fine gain 0.6 Shaping time 2 μs
Single channel analyser	Ortec 550	Mode 'Integral' Bipolar input from main amplifier
Width/Delay	NPL unit DHP 62	Width fixed at 10 μs Delay set to minimum
EHT	Tennelec TC 953	Set to +800 V

The discriminator level was set by viewing the unipolar output from the main amplifier using a multi-channel analyser (MCA) and gating the analyser with the signal from the width/delay unit. The level was set in the well defined 'valley' between the noise/photon signal and the lower end of the neutron distribution. After the level was set the counts from the SP9 counter was recorded on a scaler system, in conjunction with the signals from the various monitors. The position of the discriminator level was checked at regular intervals, by viewing the gated spectrum on the MCA, but there was no evidence of any drifting. Because the count rate in the 'valley' region is so low, any slight drifting of the discriminator introduces a negligible effect on the recorded counts from the SP9 counter.

The width/delay unit which is located in the counting chain between the single channel analyser and the scaler had a fixed, non-extending, width of 10 μs. This defines an accurate dead-time for the counting chain since this width is longer than the dead time in any preceding unit. Because of the low count rates dead-time corrections were almost negligible.